Frustrated Soft Modes and Negative Thermal Expansion in ZrW_2O_8

D. Cao,[1] F. Bridges,[1] G. R. Kowach,[2] and A. P. Ramirez[3]

[1]*Physics Department, University of California, Santa Cruz, California 95064*
[2]*Agere Systems, 600 Mountain Avenue, Murray Hill, New Jersey 07974*
[3]*MS-K764, Los Alamos National Laboratory, Los Alamos, New Mexico 87545*
(Received 10 June 2002; published 4 November 2002)

Negative thermal expansion (NTE) in cubic ZrW_2O_8 has generated much interest due to its large, isotropic, and temperature independent behavior. Here, x-ray absorption fine structure data are presented for various atom pairs, providing evidence that the low-energy modes causing NTE correspond to the correlated vibrations of a WO_4 tetrahedron and its three nearest ZrO_6 octahedra. This involves translations of the WO_4 as a rigid unit along each of the four $\langle 111 \rangle$ axes. The interconnectivity of these modes prevents an anisotropic soft mode from developing, a new geometrical phenomenon that we call the "frustrated soft mode."

ZrW_2O_8 has attracted considerable attention recently due to its large isotropic negative thermal expansion (NTE) over a wide range of temperature (from 10 to 1050 K) [1]. This behavior appears to be driven [2–4] by two optical modes with extraordinarily low energy that have been observed in specific heat measurements [2] and have a negative Grueneisen parameter [3,5]. It was proposed that the rotations of rigid WO_4 and ZrO_6 polyhedra are responsible for NTE in ZrW_2O_8, which involve a large transverse motion of the O atom in the W-O-Zr linkage [1,6,7]. However, the unusually low energy of the modes suggests that heavy atoms must be involved, not just O motion. In addition, this model does not provide any explanation as to why a soft-mode displacive transition does not occur, although both the low-energy modes and open structure in ZrW_2O_8 suggest that such a transition might take place. Indeed, a close structural relative, ZrV_2O_7, exhibits a symmetry-lowering transition where its NTE vanishes [8]. The absence of such a phase transition in ZrW_2O_8 is a question of fundamental significance, and one of us has argued for its connection to the problem of geometrical frustration in triangular magnets [9]. Here we use the x-ray absorption fine structure (XAFS) technique to investigate the local structure in this material, and from that we can extract important information about the low-energy vibration modes and therefore address the origin of NTE in this material.

XAFS data at the W L_{III}- and Zr K edges were collected as a function of temperature at the Stanford Synchrotron Radiation Laboratory (SSRL) using a powder ZrW_2O_8 sample. The energy-space data were reduced using standard procedures and the resulting k-space data were Fourier transformed (FT) to r space to show the peaks that correspond to different shells of neighbor atoms (see Fig. 1). The amplitude of the nearest neighbor W-O peak in r space has almost no temperature dependence from 20 to 315 K which supports the concept of a rigid unit for the WO_4 tetrahedra. However, the nearest Zr-O peak ampli-

tude decreases about 10% at 300 K; consequently, the ZrO_6 octahedra are stiff but clearly not rigid. A more surprising result is that the W-O-Zr linkage is also quite stiff with almost no drop in amplitude from 20 to 160 K and only a small drop in amplitude ($\sim 25\%$) as the temperature is increased to 315 K. In striking contrast, the r-space peak amplitudes for both the shortest W(1)-W(2) and the Zr-Zr atom-pair linkages decrease rapidly with temperature ($> 60\%$ decrease at 300 K).

Quantitatively the width σ of the atom-pair distribution function provides information about local distortions, including thermal vibrations and static distortions. σ is determined by fitting the r-space data to a sum of theoretical functions calculated using the FEFF7 program [10]. The σ^2 vs T plots (Fig. 2) confirm the above qualitative observations. σ_{Zr-O}^2 for the Zr-O bond increases about 50% at 300 K (ZrO_6 octahedra are stiff but non-rigid) and σ_{W-Zr}^2 for the W-Zr linkage (including multiple scattering paths) shows a comparable temperature dependence. Clearly, however, the large increase of σ^2 between 20 and 300 K for the nearest W(1)-W(2) and Zr-Zr atom pairs shows that these heavy atom vibrations have lower energies (Einstein temperature from XAFS ~ 46 K). A very important additional feature in Fig. 2 is the cusp above 100 K for the W-W and Zr-Zr pairs; this indicates a hardening of the dominant vibration frequency above 100 K and serves as a signature to connect these vibrations with the lowest Einstein mode observed in the phonon density of states [5]. Since the nearest $W(1)O_4$-$W(2)O_4$ pair is oriented along a $\langle 111 \rangle$ axis, there must be significant translations of the WO_4 unit (a correlated motion of W and O atoms) along this axis.

Because the transverse O model has been invoked by several groups [1,6,7] to explain NTE, we consider in detail the implications of this motion for the XAFS analysis. We first assume that the W-O and Zr-O bonds are completely rigid. Then to achieve the required NTE (-9×10^{-6} K^{-1}) via a transverse O vibration would
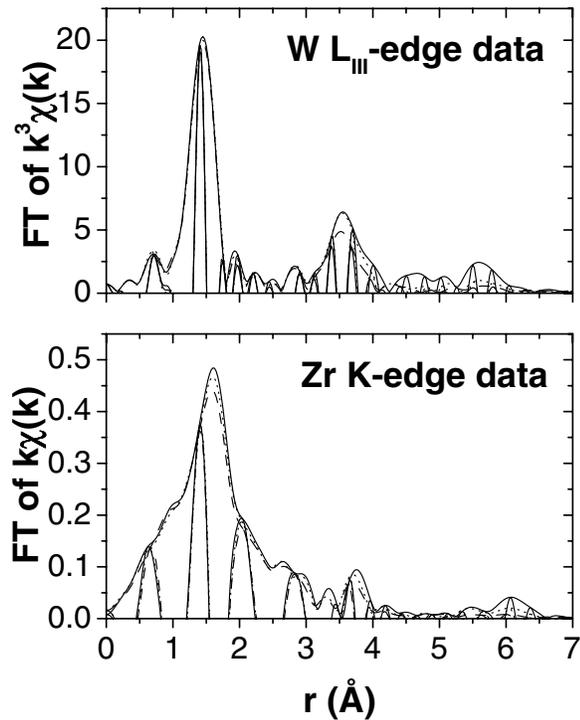
FIG. 1. XAFS r-space data for both W L_{III}- and Zr K-edge data up to 7 Å. Data at 20 K (solid line), 160 K (dotted line), and 315 K (dashed line) are shown for each edge. The Fourier transform (FT) range is from 3.3 to 13.5 Å^{-1}, with 0.3 Å^{-1} Gaussian broadening. The high frequency curve inside the envelope is the real part of the Fourier transform (FT_R). The envelope is defined as $\pm\sqrt{FT_R^2 + FT_I^2}$, where FT_I is the imaginary part of the transform. There is a well-defined XAFS phase shift for each peak, consequently the nearest W-O peak occurs at $\sim$1.4 Å (upper panel), the nearest W-Zr peak (including W-O-Zr multiple-scattering contribution) shifts to about 3.5 Å, and the nearest W-W peak is around 3.9 Å. In the bottom panel, the nearest Zr-O peak is at 1.6 Å; the nearest Zr-W peak (including Zr-O-W linkage) shifts to about 3.75 Å; the nearest Zr-Zr peak is near 6.0 Å.

require a large O vibration amplitude (about 0.20 Å; rms 0.15 Å [7]) at 300 K. Under the above assumptions, this transverse O vibration would produce a significant fluctuation of the W(1)-Zr distance [$\Delta\sigma_{W(1)-Zr}^2 \sim 0.0035$ Å^2; W(1)-O-Zr bond angle $\sim$154°), and a large change in the multiple-scattering contribution which dominates [11] for the nearly collinear linkage W(2)-O-Zr (bond angle $\sim$173°). As a result, this would lead to a $\sim$27% amplitude reduction for the W-Zr peak. However, the Zr-O bond length fluctuation will also broaden the W-Zr peak and reduce the amplitude. If we assume the transverse O vibration amplitude is zero, then the observed fluctuation of the Zr-O bond alone would reduce the W-Zr peak amplitude by $\sim$17%–20%. If the transverse O vibration and the stretching of the Zr-O bond are uncorrelated (i.e., $\sigma_{W-Zr}^2 = \sigma_{stretch}^2 + \sigma_{transverse}^2$), the overall amplitude reduction of the W-Zr peak would be $\sim$50% when we
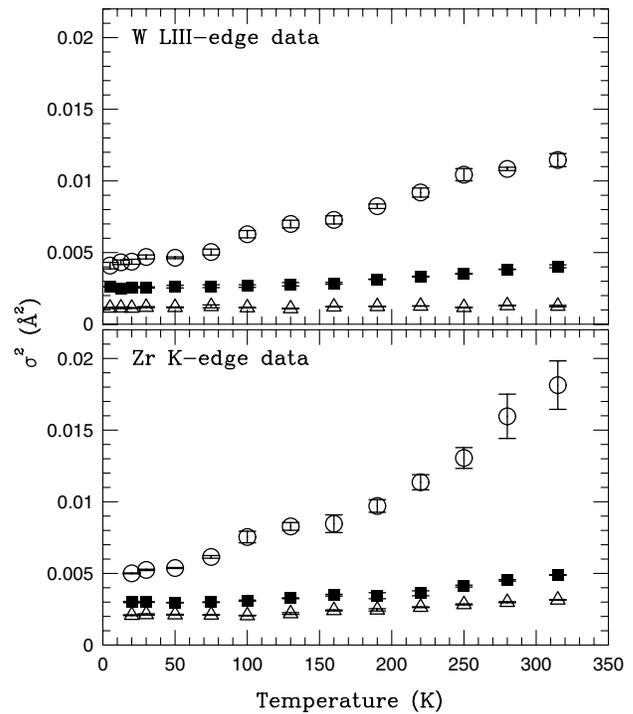

FIG. 2. σ^2 vs temperature. The W L_{III}-edge data are plotted in the upper panel: the open triangles represent the nearest neighbor W-O bonds; the solid squares show σ^2 for the W-Zr pair including W-O-Zr multiple-scattering effects; the open circles represent the nearest W(1)-W(2) atom pair. In the lower panel, σ^2 for three atom pairs are shown: the nearest neighbor Zr-O bond (open triangle), the nearest Zr-W pair including the Zr-O-W linkage (solid square), and the nearest Zr-Zr pair (open circle). Note the unusual cusp for the W-W and Zr-Zr pair data near 100 K.

include both effects, which is far too large comparing to the observed 25% reduction. This means that the atomic motions must be correlated. Since the XAFS results show that fluctuations of the W-Zr distance are small, the W and Zr motions must be partially correlated (i.e., the W-Zr pair moves as a stiff dumbbell).

Three important points emerge from the above analysis. (i) The ZrO$_6$ is not a rigid unit and the Zr-O and W-Zr distances have comparable stiffness, thereby invalidating the purely rigid unit model for ZrW$_2$O$_8$. (ii) The large thermal changes in σ^2 for both the nearest W-W and Zr-Zr pairs (Fig. 2) are good evidence that the vibrations of these atom pairs are responsible for the observed low-energy modes. (iii) The cusp above 100 K for σ_{W-W}^2 and σ_{Zr-Zr}^2, indicative of a hardening of the mode, confirms this identification (details in a longer paper).

We now construct a simplified local model for the low-frequency vibrational eigenmodes that not only explains the above XAFS data, but also accounts for the NTE. First note that the stiff W-O-Zr linkage connects the motions of a WO$_4$ tetrahedron and its three nearest ZrO$_6$ octahedra which lie in a plane perpendicular to the $\langle 111 \rangle$ axis

[Fig. 3(a)]. We use a simplified model (with O omitted) to explain the correlated motions of W and Zr based on the stiffness of W-O-Zr [Fig. 3(b)]. Consider the W atom to be at the top of a small triangular tent (but initially in the plane of the Zr) with rigid poles connected to the three Zr atoms on the base. When W moves out of the plane [as in Fig. 3(b)], then, due to the three rigid legs, the Zr-Zr distance $D_{\text{Zr-Zr}}$ will decrease and the base area must shrink while preserving the equilateral shape. A similar contraction occurs if the W moves down out of the plane. The lattice constant of ZrW_2O_8 ($a = 9.1494$ Å [12]) is directly related to $D_{\text{Zr-Zr}}$ ($a = \sqrt{2}D_{\text{Zr-Zr}}$) since the Zr atoms occupy the fcc positions in a cube. As the temperature increases, $D_{\text{Zr-Zr}}$ will on average become shorter due to the increased vibration amplitude of WO_4 along a $\langle 111 \rangle$ axis; thus, we expect to have a lattice contraction that increases with T.

A natural question that arises out of the above discussion is why does a low-energy optical mode not soften (vibration frequency goes to zero) such that a soft-mode displacive phase transition takes place? For a cubic system, there should be four equivalent vibrational modes (per unit cell) in the above model, oriented along each of the possible $\langle 111 \rangle$ axes. However, such a fourfold degeneracy is inconsistent with cubic symmetry and the actual eigenmodes must therefore be linear combinations of displacements along different $\langle 111 \rangle$ axes. This implies that the motion of the W and Zr for vibrations of the W along a given $\langle 111 \rangle$ axis are coupled to other $\langle 111 \rangle$ axes. This frustrates a possible soft-mode transition. Using group theory, we can write down the local modes that are consistent with space group $P2_13$. Let $a_{1,1,1}$ represent a vibration amplitude of W-W along the $[1, 1, 1]$ axis. Then under the 12 symmetry operation for $P2_13$, this amplitude will be transformed to a vibration along one of the other three $\langle 1, 1, 1 \rangle$ axes (or remain unchanged). There are four possible linear combinations of these amplitudes—three of which are degenerate and transform into each other.

Singlet:

$$\Psi_1 = 0.5(a_{1,1,1} + a_{-1,1,1} + a_{1,1,-1} + a_{1,-1,1}). \quad (1)$$

Triplet:

$$\begin{aligned}
\Psi_2 &= 0.5(a_{1,1,1} + a_{-1,1,1} - a_{1,1,-1} - a_{1,-1,1}), \\
\Psi_3 &= 0.5(a_{1,1,1} - a_{-1,1,1} - a_{1,1,-1} + a_{1,-1,1}), \quad (2) \\
\Psi_4 &= 0.5(a_{1,1,1} - a_{-1,1,1} + a_{1,1,-1} - a_{1,-1,1}).
\end{aligned}$$

For each mode Ψ, there are equal amplitudes along each of the $\langle 1, 1, 1 \rangle$ axes and hence equal contractions in all directions. Thus, if one of these modes were to become frozen it would not change the symmetry—there is no preferred direction. The analysis of David et al. [3] indicates that the lowest mode at 3.3 meV (singlet) has by far the most negative Grueneisen parameter [a factor of 20 larger in magnitude than that for the 5.8 meV mode (triplet), and hence dominates for NTE].

The coupling between different axes which frustrates a soft-mode transition can be understood geometrically. In Fig. 3 we showed that the triangles around each W atom would shrink uniformly as W vibrates transversely; we now consider the consequences of such displacements for the entire lattice. Figure 4 shows three (of the four possible) planes which are perpendicular to different $\langle 111 \rangle$ axes. First let us focus on the white plane in panels 1 and 2. Note that the structure contains both filled Zr triangles (with W atoms in the center) and nonfilled Zr triangles. The latter form hexagons (panel 2 of Fig. 4) in this kagome lattice; similar patterns are found for other $\langle 111 \rangle$ planes. If the W atoms vibrate transversely to the white plane, then each of the filled triangles will contract uniformly (panel 2 of Fig. 4). This will in turn contract the hexagon in the center and preserve its equilateral shape as the central Zr is constrained by the lattice against a large vertical displacement, although the Zr atom can move within the planes. Consequently, the nonfilled triangles also shrink, which then drives vibrations of the W atoms perpendicular to other $\langle 111 \rangle$ planes as depicted in panel 3 of Fig. 4. Thus, a shrinkage in one plane is coupled to a local shrinkage on each of the other $\langle 111 \rangle$ planes.

The interconnectivity of the $\langle 111 \rangle$-type motions illustrates why these displacements can be soft locally, yet resist a symmetry-lowering phase transition. An analogy to this local motion is found in the "Hoberman$^{\text{TM}}$ sphere," a children's toy which retains its spherical shape while changing size in response to a uniaxial force. The dynamics of a related two-dimensional version of this model are discussed by Simon and Varma [13]. A similar mechanism seems to be operative in ZrW_2O_8 on the nanometer scale and explains how ZrW_2O_8 retains its cubic
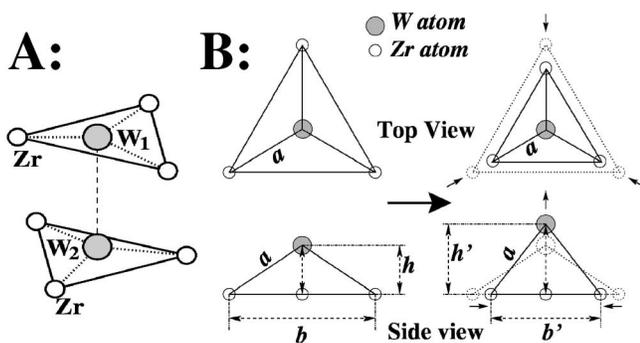

FIG. 3. (a) A simplified drawing of part of the structure which shows three nearest Zr atoms in a triangle surrounding either the W(1) or W(2) atoms. See Fig. 4 for the structure over a larger scale. (b) A rigid-tentpole model to show the constraint on the correlated motions between a W atom and it nearest Zr atoms. As W moves up (right side of the figure), the Zr must move together to keep the W-Zr linkage rigid. This leads to a net lattice contraction.
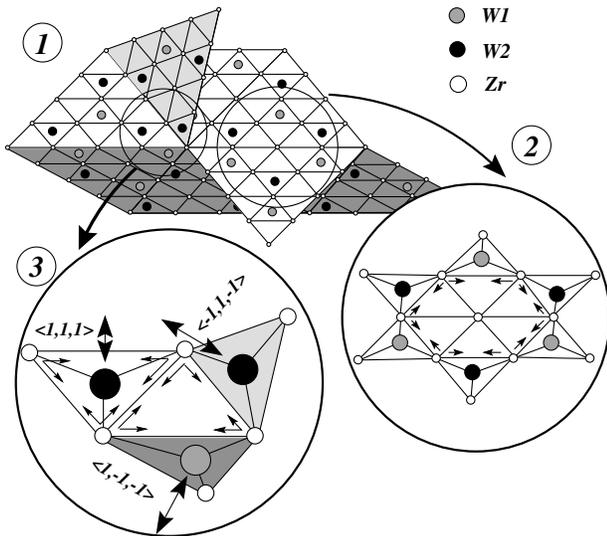
FIG. 4.   A sketch of part of the crystal structure with only W and Zr atoms plotted (O atoms are omitted for clarity). The white, light gray, and dark gray planes are three different planes perpendicular to $\langle 1, 1, 1 \rangle$, $\langle -1, 1, -1 \rangle$, and $\langle 1, -1, -1 \rangle$ axes, respectively. Zr atoms are at the corner of each triangle, while W atoms are at the center of every thick-line triangle (filled triangle). Panels 2 and 3 show the detailed structure of small parts of panel 1, in which the W-O-Zr linkage is shown by a thin black solid line. Panel 2 shows part of the white plane with six connected filled triangles surrounding a hexagon formed by six nonfilled triangles. The thick arrows in panel 3 show the vibration direction of each W atom.

structure. Presumably, further neighbor interactions limit the size change in response to thermal vibrations. Interestingly, the Hoberman$^{\text{TM}}$ sphere is an example of a system with a negative Poisson ratio, a quantity which measures the transverse expansion in response to a uniaxial compression. It remains to be seen whether or not the local motion found in ZrW_2O_8 is manifested as a negative Poisson ratio in the bulk.

In conclusion, the WO_4 tetrahedra are essentially rigid over a wide temperature range (5 to 315 K) but the ZrO_6 octahedra are not, although the Zr-O bonds are quite stiff. Importantly, the W-Zr linkage between these two types of polyhedra has a comparable stiffness to Zr-O and the W-Zr pair will move as a unit to the same extent as the ZrO_6 unit; consequently, some of the O motion must be related to translations of WO_4 and ZrO_6. Thus, transverse vibrations of O in the W-O-Zr linkage cannot be the primary origin of NTE in this material. The XAFS results indicate that the vibrations of the nearest W and Zr atom are correlated with a translation of WO_4 along a $\langle 111 \rangle$ axis; the W(1)-W(2) and Zr-Zr pairs have the lowest vibrational energy with a hardening of the vibration frequency near 100 K. These correlated displacements suggest the form of the eigenmodes that lead to NTE. The coupled motions along different $\langle 111 \rangle$ axes also frustrate the formation of a soft-mode transition; consequently, the lattice shrinks uniformly along all four $\langle 111 \rangle$ axes, which maintains the cubic lattice structure.

[1] T. A. Mary, J. S. O. Evans., T. Vogt, and A. W. Sleight, Science **272**, 90 (1996).
[2] A. P. Ramirez and G. R. Kowach, Phys. Rev. Lett. **80**, 4903 (1998).
[3] W. I. F. David, J. S. O. Evans, and A. W. Sleight, Europhys. Lett. **46**, 661 (1999).
[4] R. Mittal and S. L. Chaplot, Solid State Commun. **115**, 319 (2000).
[5] G. Ernst, C. Broholm, G. R. Kowach, and A. P. Ramirez, Nature (London) **396**, 147 (1998).
[6] A. K. A. Pryde *et al.*, J. Phys. Condens. Matter **8**, 10 973 (1996).
[7] J. S. O. Evans, W. I. F. David, and A. W. Sleight, Acta Crystallogr. Sect. B **B55**, 333 (1999).
[8] V. Korthuis *et al.*, Chem. Mater. **7**, 412 (1995).
[9] A. P. Ramirez, in *Handbook of Magnetic Materials*, edited by K. H. J. Buschow (North-Holland, Elsevier Science B.V., Amsterdam, 2001), p. 423.
[10] S. I. Zabinsky, J. J. Rehr, A. Ankudinov, R. C. Albers, and M. J. Eller, Phys. Rev. B **52**, 2995 (1995).
[11] *X-Ray Absorption Principles Applications Techniques of EXAFS SEXAFS XANES*, edited by D. Koningsberger and R. Prins (Wiley, New York, 1988).
[12] J. D. Jorgensen, Z. Hu, S. Teslic, D. N. Argyriou, S. Short, J. S. O. Evans, and A. W. Sleight, Phys. Rev. B **59**, 215 (1999).
[13] M. E. Simon and C. M. Varma, Phys. Rev. Lett. **86**, 1781 (2001).